International Journal of Heat and Mass Transfer 106 (2017) 816–828

Contents lists available at ScienceDirect

International Journal of Heat and Mass Transfer

journal homepage: www.elsevier.com/locate/ijhmt

Forced convective heat transfer of nanofluids around a circular bluff body with the effects of slip velocity using a multi-phase mixture model

R. Deepak Selvakumar, S. Dhinakaran *

The Center for Fluid Dynamics, Discipline of Mechanical Engineering, Indian Institute of Technology Indore, Khandwa Road, Simrol, Indore 453 552, MP, India

ARTICLE INFO

Article history:
Received 10 June 2016
Received in revised form 26 September 2016
Accepted 30 September 2016
Available online 4 November 2016

Keywords:
Circular cylinder
Nanofluids
Multi-Phase Modeling (MPM)
Mixture model
FVM
Slip velocity

ABSTRACT

Forced convective heat transfer around a circular cylinder using nanofluids has been numerically analyzed employing a mixture model based Multi-Phase Modeling (MPM) approach. A hot circular cylinder with a constant wall temperature is exposed to a free stream of Al_2O_3–H_2O nanofluid at ambient temperature. The flow is steady, laminar and two dimensional in the Reynolds number range of $10 \leqslant Re \leqslant 40$. The governing equations of flow and energy transfer along with the respective boundary conditions are numerically solved using a Finite Volume Method (FVM) based on SIMPLE algorithm. The prime aim of this work is to highlight the effects of slip velocity, volume concentration and diameter of nanoparticles on heat transfer characteristics of nanofluids. Results indicate that heat transfer increases with increase in nanoparticle volume fraction. The highest mean Nusselt number is observed at $\phi = 5\%$ at any Reynolds number. It is also noted that, nanofluids with smaller nanoparticles result in higher heat transfer rates. Particular attention has been paid to the variation of heat transfer characteristics when the modeling approach is switched from Single-Phase Modeling (SPM) to mixture model based MPM. It is revealed that higher heat transfer rates are observed in MPM which considers the effects of slip velocity.

1. Introduction

Forced convective heat transfer around bluff bodies is a frequently encountered scenario in many industrial applications such as cooling of electronic components, nuclear reactors, shell type heat exchangers, pin fins and use of thin wires as probes and sensors, etc [1]. In addition to these practical applications, this scenario is also a classical problem in fluid mechanics and heat transfer. A considerable volume of information on various flow phenomena observed in this flow configuration has accumulated in literature over the years. Excellent review articles and books consolidating the current state of the art of fluid flow and heat transfer over a circular cylinder are now available in literature [2–10]. However, the heat transfer performance in engineering applications is limited by the low thermal conductivity of traditional industrial coolants such as air, water, engine oil and ethylene glycol. Nanofluids which are obtained by suspending fine nano-sized particles in conventional cooling liquids are the new generation coolants with enhanced thermal conductivity and good stability. They find applications in electronic component cooling, automobiles, nuclear reactors, energy storage and solar absorbers, etc [11]. Hence, several experimental and numerical research attempts are in progress to utilize nanofluids in thermal applications to achieve enhanced heat transfer performance.

In recent years, several numerical investigations on nanofluid flow and heat transfer around bluff bodies have been reported in literature. Nanofluids due to their different effective thermophysical properties exhibit modified flow and heat transfer characteristics. Valipour and Ghadi [12] numerically analyzed the forced convective heat transfer around a solid circular cylinder using nanofluids. The effective thermal conductivity and viscosity of nanofluids were determined using Hamilton-Crosser model [13] and Brinkman model [14], respectively. Nanofluids exhibited stronger vorticity and enhanced heat transfer rates. A similar study on forced convective heat transfer past a square cylinder by Valipour et al. [15] also confirmed their observations on circular cylinder. A numerical study on forced convective nanofluid flow around a circular cylinder by Vegad et al. [16] in which the effective properties were calculated using Maxwell Garnett model [17] and Brinkman model [14] also showed synonymous results. Abu-Nada et al. [18] in their numerical study on mixed convective heat transfer around a circular cylinder showcased that the heat transfer enhancement is dependent on thermal conductivity of nanoparticles and particle volume fraction. Bing and Mohammed [19] performed a numerical study on upward laminar mixed convective flow around a circular cylinder and showed that nanofluids with smaller nanoparticles produced higher heat transfer rates.

* Corresponding author.
E-mail address: ssdhinakar@gmail.com (S. Dhinakaran).

http://dx.doi.org/10.1016/j.ijheatmasstransfer.2016.09.108
0017-9310/

Nomenclature

Notations

a	acceleration [m/s^2]
c_p	specific heat capacity [J/kg K]
D	diameter of the cylinder [m]
d_f	basefluid molecular diameter [m]
d_p	diameter of the nanoparticle [m]
f_{drag}	drag function
H	enthalpy [J/kg]
k	thermal conductivity [W/m K]
Nu	Nusselt number
P	pressure [N/m^2]
T	temperature [K]
Pr	Prandtl number
Re	Reynolds number
V,v	velcoity components [m/s]

Greek symbols

μ	dynamic viscosity [kg/ms]
v	kinematic viscosity [m^2/s]
ϕ	nanoparticle volume fraction
ρ	density [kg/m^3]

Subscripts

dr	drift velocity
f	basefluid (primary phase)
M	mean value
m	mixture
nf	nanofluid
p	nanoparticle (secondary phase)
pf	slip velocity
S	local value
s	phase

Farooji et al. [20] numerically simulated a laminar nanofluid flow around a circular cylinder and exhibited that there is an optimum particle volume fraction for a given nanoparticle diameter at which the maximum heat transfer will be observed. A numerical analysis of transient natural convective boundary layer flow past a vertical cylinder using nanofluids by Chamkha et al. [21] showcased the dependence of heat transfer enhancement on nanoparticle shape. It was noted that spherical particles are capable of producing higher heat transfer rates. Notable aspect of this work is that Brownian motion and thermophoresis were considered while determining the effective thermal conductivity of nanofluids. Sarkar et al. [22] made a detailed study on wake dynamics and heat transfer using nanofluids in forced and mixed convective flow past a circular cylinder at high Prandtl numbers. A stabilizing effect in flow and enhanced heat transfer were noted at higher Richardson numbers. Similar results were obtained in a numerical study of mixed convective flow around a circular cylinder using nanofluids [23]. A buoyancy driven mixed convective flow around square cylinder using nanofluids by Sarkar et al. [24] showed that heat transfer is a function of particle volume fraction. Addition of nanoparticles to the basefluid resulted in more number of low frequency higher energy modes in a mixed convection flow around a square cylinder [25]. During a mixed convective vertical flow and heat transfer around a square cylinder using nanofluids, addition of nanoparticles to the basefluid caused a decrease in total entropy generation [26].

It is to be noted that all the available works on nanofluid flow around cylindrical bodies are based on a Single-Phase Modeling (SPM) approach. In SPM, it is assumed that nanofluids are homogeneous fluids with effective properties. The effective properties are calculated using theoretical models and it is considered that the nanoparticles and liquid move with the same velocity. It is also hypothesized that the particles and basefluid are in thermal equilibrium. This approach is simpler and computationally less expensive. In reality, nanofluids are heterogeneous suspensions consisting of randomly moving particles and a continuous fluid phase. Factors and mechanisms such as gravity, friction between the fluid and solid particles, thermophoresis, Brownian motion, the phenomena of Brownian diffusion, sedimentation and dispersion may exist along with the main flow of nanofluid. Also, the difference in density of nanoparticles and fluid may cause a difference of velocity between both the phases. These factors indicate that the fluid and particles will not have same velocity and there will be a velocity slip between them [27]. Hence, it is obvious that Multi-Phase Modeling (MPM) approach is more suitable for modeling flow and convective heat transfer of nanofluids. In MPM, dynamics of each phase is explicitly considered and it aids in understanding the behavior of fluid phase and solid particles in the heat transfer process [28]. There are two MPM approaches for modeling the flow of solid–liquid mixtures [29,30], namely the Lagrangian–Eulerian approach and Eulerian–Eulerian approach. Lagrangian–Eulerian approach analyses the fluid phase using the Eulerian model and the solid particles are analyzed using a Lagrangian approach. This approach is suitable only when the solid particle volume fraction is less. In nanofluids, the number of particles is extremely high due to very small size of nanoparticles. Hence, Lagrangian–Eulerian approach is not economic for solving nanofluid flow problems due to software limitations, memory, time and CPU requirements, etc. The second approach is Eulerian–Eulerian approach which considers the particle phase as continuum and is more suitable for nanofluid problems [31]. There are three different Eulerian–Eulerian models which are more popularly used for solving nanofluid problems, namely (i) VOF (Volume of Fluid), (ii) Mixture and (iii) Eulerian [28,32–51]. Out of the three Eulerian models, mixture theory which is also known as the theory of interacting continua [31,52–54] is more popular due to its simplicity in theory and implementation. The mixture model considers the mixture as a whole, instead of two separate phases and hence, it is straightforward, relatively inexpensive and considerably accurate for a wide range of multi-phase flows [52].

For the first time in literature, Behzadmehr et al. [32] employed the Eulerian-mixture model to predict the forced convective heat transfer in a circular tube using Cu–Water nanofluids. It was observed that, mixture model produced more accurate results than SPM and matched well with the experimental results. Mirmasoumi and Behzadmehr [39] utilized mixture model to numerically study the mixed convective heat transfer of nanofluids through a horizontal tube. It was observed that the thermal parameters are notably influenced by the nanoparticle distribution and higher concentration of nanoparticles was observed at the bottom and near wall region. Laminar flow of nanofluids in a curved tube was numerically studied by Akbarinia and Laur [28] using mixture model. Effects of particle diameter have been exclusively analyzed and it was concluded that increasing the particle diameter increases the axial velocity and decreases the Nusselt number. Also, an uniform distribution of nanoparticles was observed all over the tube. A mixture model based numerical study was carried out by Alinia et al. to investigate the mixed convection heat transfer inside a two sided lid driven cavity filled

with nanofluids [33]. In addition to the effects of inclination, significant increase in heat transfer inside the cavity and modifications in flow pattern were observed due to addition of nanoparticles. Turbulent intensity and thermal parameters were found to be significantly affected by the variation in nanoparticle concentration in a mixture model based numerical analysis of turbulent mixed convection of nanofluids in a horizontal curved tube [35]. Goodarzi et al. [37] employed mixture model to study the mixed convection heat transfer of nanofluids in a shallow cavity. It was noted that addition of nanoparticles resulted in augmentation of heat transfer and for a given Grashof number, higher heat transfer rates were observed at lower Richardson numbers. Lotfi et al. [38] performed a comparative study of different modeling approaches to analyze forced convective nanofluid flow and heat transfer in a horizontal tube. It was inferred that mixture model produced results which were matching closely with experimental data. Moghari et al. [40] applied mixture model to study the mixed convection heat transfer of nanofluids inside a circular annulus. Addition of nanoparticles resulted in significant augmentation of heat transfer whereas, the skin friction coefficient was showing only a marginal increase. Pakravan and Yaghoubi [41] analyzed the migration of nanoparticles in a closed square cavity using mixture model. It was clearly shown that single phase assumption of nanofluids is not valid for a natural convective scenario. Heat transfer and entropy generation of turbulent forced convective nanofluid flow in a horizontal tube was studied by Saha and Paul [42] using mixture model. It was noted that mixture model based multiphase approach produced higher heat transfer rates than the Single-Phase Modeling approach. More recently, Esfiandry et al. [34] numerically examined the natural convective heat transfer behavior of nanofluids inside an enclosure using mixture model. It was clearly observed that the inclusion of slip velocity mechanisms in the mixture model notably influences the heat transfer characteristics. Also, recent review articles on modeling approaches for convective heat transfer of nanofluids [55,56] indicate that single-phase approach is not suitable for nanofluids and produces results that vary from experimental data. It is also revealed that Eulerian–Eulerian approach based on mixture model is capable of producing sufficiently accurate results with less computational expense.

From the above literature review, it is observed that all available works on nanofluid flow around circular/square cylinders follow a single phase approach. To the best of the knowledge of authors, this is the first study to numerically analyze the nanofluid flow and heat transfer around a circular cylinder using Multi-Phase Modeling (MPM) based on Eulerian-mixture model. Engineering problems involving flow and heat transfer of nanofluids often require the understanding of behavior of total mixture rather than individual constituent phases. Hence, mixture model is chosen for this study. The prime aim of this study is to highlight the effects of particle volume fraction, particle diameter and Reynolds number on heat transfer characteristics of Al_2O_3-H_2O nanofluids using an Eulerian-mixture model which considers the effects of slip velocity between the nanoparticles and basefluid. A 2-D, steady, laminar and forced convective flow is considered with the Reynolds number varying from 10 to 40. The particle volume fraction is varied in the range of $0\% \leqslant \phi \leqslant 5\%$ and the particle diameters of 10, 20, 30, 40 and 50 nm are considered. Particular attention is paid to the heat transfer characteristics and the variation in heat transfer enhancement if the modeling approach is switched from SPM to MPM.

2. Problem definition and mathematical formulation

An infinitely long cylinder of circular cross section with diameter D is considered. The hot cylinder is considered to be at a Constant Wall Temperature (CWT) and exposed to nanofluid flowing with an uniform velocity and at ambient temperature. Center of the cylinder is considered to be at the origin of a cylindrical coordinate system and the uniform stream of nanofluid is directed towards positive x-direction. The flow is considered to be two-dimensional as the cylinder is infinitely long. The cylinder is considered to exchange heat with the surrounding nanofluid stream. The outer boundary is placed at a sufficient distance $50D$ away from the cylinder surface in order to make the problem computationally feasible. A schematic diagram of the flow domain is shown in Fig. 1(a).

2.1. Governing equations

The nanofluid flow and heat transfer is modeled using an Eulerian-mixture model. Eulerian-mixture model which is based on a single fluid two-phase approach considers the phases (basefluid and nanoparticles) to be strongly coupled and the secondary phase (particles) closely follow the flow. The notable feature of this

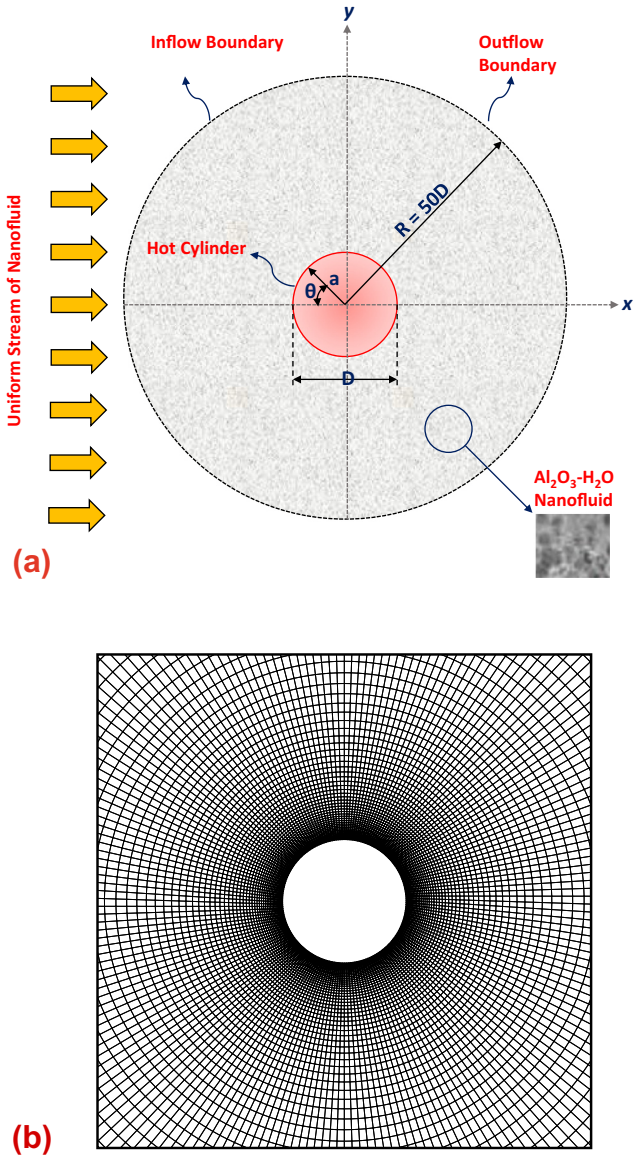

Fig. 1. (a) Schematic representation of the flow domain and (b) Close view of the mesh.

approach is that only a single set of velocity elements is solved for the mixture momentum conservation equations. The velocity of the secondary phase is extracted from the algebraic formulations [57]. The phases are assumed to be inter-penetrating with each other (i.e.,) each phase has its own vector velocity field and is represented by its own volume concentration within any control volume. Both the phases are assumed to share a single pressure. Furthermore, the primary phase influences the secondary phase by means of drag force and the effect of secondary phase on primary phase can be calculated by means of mean momentum reduction. Instead of utilizing the governing equations of each phase separately, the continuity, momentum and energy equations are solved for the mixture and only the volume fraction equation is solved for secondary phase (nanoparticles). The concentration of the secondary dispersed phase (nanoparticles) is solved by a scalar equation, considering the correction made by phase slip. The governing equations of fluid flow and heat transfer for multi-phase mixture model in dimensional form are presented with the following assumptions [38,58].

- The fluid flow is incompressible, laminar and Newtonian.
- The Boussinesq approximation is negligible.
- Nanoparticles are spherical, uniform in size and shape.
- The viscous dissipation is very negligible.

Continuity equation:

The continuity equation for the mixture is

$$\nabla \cdot \left(\rho_m \vec{V}_m\right) = 0 \tag{1}$$

where, $\vec{V}_m$ is the mass averaged velocity of the mixture (nanofluid).

Momentum equation:

The mixture momentum equation is obtained by summing the individual momentum equations of every phase and is expressed as

$$\nabla \cdot \left(\rho_m \vec{V}_m \vec{V}_m\right) = -\nabla P_m + \nabla\left[\mu_m \nabla \vec{V}_m - \sum_{s=1}^{n} \phi_s \rho_s \overline{v}_s \overline{v}_s\right] + \nabla \cdot \left(\sum_{s=1}^{n} \phi_s \rho_s \vec{V}_{dr,s} \vec{V}_{dr,s}\right) \tag{2}$$

Here, n is the number of phases and μ_m is the mixture (nanofluid) viscosity

Energy equation:

The energy equation of the mixture takes the following form

$$\nabla \cdot \left[\sum_{s=1}^{n} \phi_s \vec{V}_s (\rho_s H_s + P_m)\right] = \nabla \cdot \left(k_m \nabla T - c_p \rho_m \overline{vt}\right) \tag{3}$$

Here, k_m is the effective thermal conductivity of the mixture.

Volume fraction equation

The volume fraction of the secondary phase is obtained as

$$\nabla \cdot \left(\phi_p \rho_p \vec{V}_m\right) = \nabla \cdot \left(\phi_p \rho_p \vec{V}_{dr,p}\right) \tag{4}$$

In the above equations, ρ_m, μ_m and k_m are the mixture density, viscosity and thermal conductivity, respectively. The mixture velocity ($\vec{V}_m$) is determined as follows:

$$\vec{V}_m = \sum_{s=1}^{n} \frac{\phi_s \rho_s \vec{V}_s}{\rho_m} \tag{5}$$

where, ϕ_s is the volume fraction of phase s and H_s is the enthalpy of phase s. In Eq. (2) $\vec{V}_{dr,p}$ is the drift velocity for the secondary phase (p) and is expressed as

$$\vec{V}_{dr,p} = \vec{V}_p - \vec{V}_m \tag{6}$$

Velocity of the secondary phase (p) in relation to the primary phase (f) is known as the relative or slip velocity and is defined as

$$\vec{V}_{pf} = \vec{V}_p - \vec{V}_f \tag{7}$$

The drift velocity is related to the slip velocity as

$$\vec{V}_{dr,p} = \vec{V}_{pf} - \sum_{s=1}^{n} \vec{V}_{pf} \frac{\phi_p \rho_p}{\rho_m} \tag{8}$$

Following equations were proposed by Manninen et al. [31] and Schiller and Naumann [59] to calculate the slip velocity ($\vec{V}_{pf}$) and drag function (f_{drag}), respectively.

$$\vec{V}_{pf} = \frac{\rho_p d_p^2}{18 \mu_f f_{drag}} \frac{\rho_p - \rho_m}{\rho_p} \vec{a} \tag{9}$$

$$f_{drag} = \begin{cases} 1 + 0.15 Re_p^{0.687}, & \text{if } Re_p \leqslant 1000. \\ 0.0183 Re_p, & Re_p > 1000. \end{cases} \tag{10}$$

In the above equation, $Re_p = (V_m d_p)/\nu_{eff}$ and the acceleration (a) is given as $a = g - (V_m \cdot \nabla) V_m$.

2.2. Boundary conditions

Suitable boundary conditions as described below are applied at the corresponding flow boundaries to numerically solve the flow problem.

Inflow boundary:

At the inflow boundary an uniform flow in x-direction and ambient temperature are assumed for both the phases.

Outflow boundary:

Convective boundary condition has been used as it decreases the number of time steps and allows smaller length of outer boundary [60].

Cylinder wall:

No-slip conditions for the velocities are applied and a constant wall temperature higher than ambient temperature is considered.

2.3. Thermo-physical properties of nanofluids

The thermo-physical properties of water (base fluid) and Alumina (nanoparticles) are provided in Table 1. Nanofluids have different effective thermo-physical properties than their base components. Numerous models are available in literature to predict the thermo-physical properties of nanofluids and there is an uncertainty prevailing in the prediction of nanofluid properties. In present study, classic formulas of Buongiorno [61] are used to determine the density and heat capacitance of nanofluids.

2.3.1. Effective density

Effective density of nanofluid is calculated as

$$\rho_{nf} = (1 - \phi)\rho_f + \phi \rho_p \tag{11}$$

In Eq. (11), ϕ is the nanoparticle volume fraction; ρ_p and ρ_f are the densities of nanoparticles and basefluid, respectively.

2.3.2. Effective heat capacitance

Effective heat capacitance of nanofluid is determined as follows:

$$(\rho c_p)_{nf} = (1 - \phi)(\rho c_p)_f + \phi (\rho c_p)_p \tag{12}$$

where, $(\rho c_p)_f$ and $(\rho c_p)_p$ are the heat capacitance of the basefluid and nanoparticles, respectively.

Table 1
Thermo-physical properties of the basefluid (water) and nanoparticles (Al_2O_3) [34].

S. No	Material	Thermal conductivity (W/m K)	Dynamic viscosity (Kg/mS)	Density (kg/m^3)	Heat capacitance (J/kg K)
1	Al_2O_3	40	–	3970	765
2	H_2O	0.6	0.001003	997	4179

2.3.3. Effective thermal conductivity

In the present study, correlation proposed by Corcione [62] is used to predict the effective thermal conductivity of nanofluids due to the lack of experimental results and correlations which relate the nanoparticle diameter and temperature to the effective properties of nanofluids. The following correlation by Corcione [62] predict the thermal conductivity of the nanofluid based on temperature, particle diameter, volume concentration and properties of the basefluid and nanoparticles.

$$\frac{k_{nf}}{k_f} = 1 + 4.4 Re_p^{0.4} Pr_f^{0.66} \left(\frac{T}{T_{fr}}\right)^{10} \left(\frac{k_p}{k_f}\right)^{0.03} \phi^{0.66} \tag{13}$$

where, Re_p is the nanoparticle Reynolds number due to Brownian motion and is given as

$$Re_p = \frac{2\rho_f K_B T}{\pi \mu_f^2 d_p} \tag{14}$$

T_{fr} is the freezing point of pure water (basefluid); K_B (1.38×10^{-23} J/K) is the Boltzmann constant; d_p is the particle diameter ($10\ \text{nm} \leqslant d_p \leqslant 150\ \text{nm}$) and T is the nanofluid temperature. ρ_f and μ_f are the density and dynamic viscosity of the basefluid, respectively.

2.3.4. Effective dynamic viscosity

The effective viscosity of nanofluids are calculated by another correlation by Corcione [62] which is given below

$$\frac{\mu_f}{\mu_{nf}} = 1 - 34.87 \left(\frac{d_p}{d_f}\right)^{-0.3} \phi^{1.03} \tag{15}$$

In Eq. (15), d_f is the diameter of basefluid molecule which is defined as

$$d_f = 0.1 \left(\frac{6M}{N\pi\rho_f}\right)^{1/3} \tag{16}$$

where, N is the Avagadro number and M is the molecular weight of basefluid.

2.4. Definitions of certain parameters

Some of the parameters used in this study are defined as follows:

2.4.1. Nusselt number

Local Nusselt number (Nu_s) at any point on the cylinder surface is given as follows:

$$Nu_s = -\frac{\partial T}{\partial n} \tag{17}$$

where, n is the cylinder surface normal direction. The mean Nusselt number (Nu_M) is calculated by averaging the local Nusselt number along the entire cylinder surface.

2.4.2. Heat transfer enhancement ratio (E)

The heat transfer enhancement produced by nanofluid with any nanoparticle volume fraction is expressed by means of heat transfer enhancement ratio (E). It is given by the ratio of mean Nusselt number of nanofluid to mean Nusselt number of pure water (basefluid).

$$E = \frac{(Nu_M)_{nf}}{(Nu_M)_f} \tag{18}$$

3. Numerical methods and grid sensitivity analysis

The computational domain is prepared, meshed and suitable boundary conditions are set using the commercial preprocessor software ANSYS ICEM CFD 15.0. The governing equations of continuity, momentum and energy along with the suitable boundary conditions are discretized and solved using the Finite Volume Method based solver Fluent 15.0. The governing equations which are non-linear partial differential equations are converted into non-linear algebraic equations. SIMPLE algorithm is employed for the pressure-velocity coupling. A third-order accurate QUICK scheme has been employed to discretize the convective terms. All equations are solved in sequential iterations to obtain a con-

Table 2
Grid sensitivity analysis using basefluid (water) as working fluid.

S. No	*Re*	Grid	C_D	% Difference	Nu_M	% Difference
Outer boundary distance = 50 D						
1	10	100×100	2.8008	0.078	3.8163	0.123
2	10	150×150	2.7986	0.003	3.8210	0.028
3	10	200×200	2.7985	–	3.8221	–
4	40	100×100	1.5154	0.131	7.0859	0.187
5	40	150×150	1.5174	0.276	7.0992	0.601
6	40	200×200	1.5132	–	7.0565	–
Outer boundary distance = 70 D						
7	10	100×100	2.7963	0.414	3.8196	0.149
8	10	150×150	2.7847	0.003	3.8139	0.031
9	10	200×200	2.7846	–	3.8151	–
10	40	100×100	1.5095	0.072	7.0962	0.207
11	40	150×150	1.5084	0.019	7.0815	0.050
12	40	200×200	1.5081	–	7.0851	–

verged solution. In the present study, all solutions are considered to be converged when the residuals become less than 10^{-6}. Extensive computations have been performed to determine the suitable grid to justify the correctness and stability of the numerical solutions. Grid sensitivity analysis was carried out by varying the number of grid points in the circumferential and radial directions, and distance of the outer boundary. Grid independence study is carried out for a particular case of water (basefluid) at Reynolds numbers 10 and 40. Three different combinations of grid with two outer boundary lengths have been considered to ensure the grid in-dependency of the solution. The results of grid sensitivity analysis are presented in Table 2. Based on the results of grid sensitivity analysis, 100×100 grid with $50D$ outer boundary distance has been selected with the consideration of computational expenses and to ensure consistent numerical results. A non-uniform grid which is more fine near the cylinder wall as shown in Fig. 1(b) is considered to capture the large variations and sharp gradients of flow field behavior near the wall.

4. Validation of numerical results

The numerical results of the present code with air as working fluid ($Pr = 0.71$) is compared with the studies available in literature at $10 \leqslant Re \leqslant 40$. In Fig. 2(a), comparison of coefficient of drag obtained from present code is compared with the results of Lange et al. [5], Dennis and Chang [63] and Soares et al. [64] is shown graphically. Fig. 2(b) graphically compares the mean Nusselt number from the present code with Soares et al. [64] and Lange et al. [5]. It is clear that the present numerical results are in good agreement with the results available in literature and hence, we can be confident of the results presented in this study.

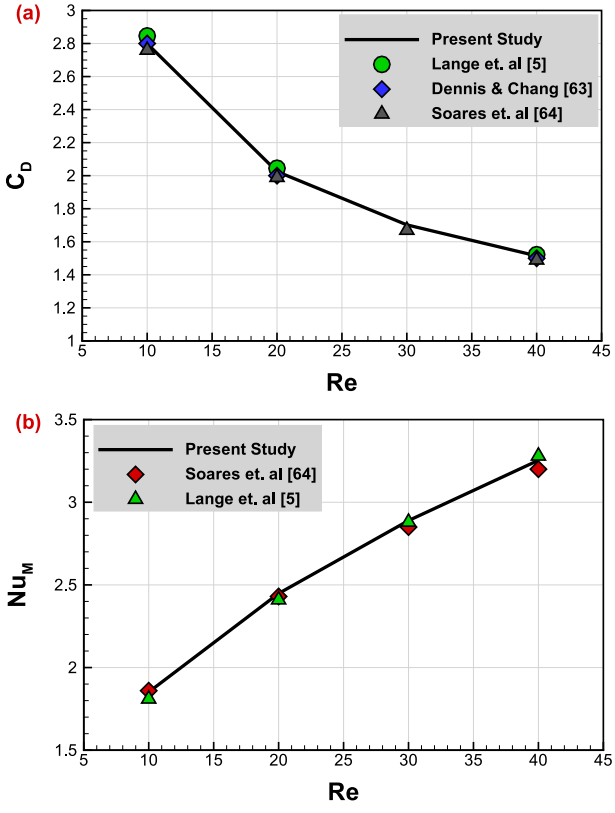

Fig. 2. Comparison of results from present code with literature for $Pr = 0.71$ (a) coefficient of drag (C_D) and (b) Mean Nusselt number (Nu_M).

5. Results and discussions

Numerical simulations of Alumina (Al_2O_3)–Water (H_2O) nanofluid flow and heat transfer around a circular cylinder is performed with the following range of governing parameters:

Reynolds number (Re)	:	10, 20, 30 and 40.
Particle volume fraction (ϕ)	:	0–5% in steps of 1.
Particle diameter (d_p)	:	10, 20, 30, 40 and 50 nm.

Results and discussion provided hereafter highlight the effects of particle volume fraction, particle diameter and slip velocity at different Reynolds numbers on heat transfer characteristics around a circular cylinder using nanofluids.

5.1. Nanoparticle volume concentration

Fig. 3 graphically presents the radial distribution of percentage volume fraction of nanoparticles along the surface of the cylinder at $10 \leqslant Re \leqslant 40$ and for different nanoparticle diameters $10\,\text{nm} \leqslant d_p \leqslant 50\,\text{nm}$. It was observed that the nanoparticle distribution is absolutely uniform along the cylinder surface. Irrespective of the particle diameter, volume fraction and Reynolds number; the distribution of nanoparticles along the surface of the cylinder remained constant. This is also an indication that the distribution of nanoparticles is almost uniform throughout the flow domain. By this observation, we can say that the assumption of uniform distribution of nanoparticles in the basefluid considered in Single-Phase Modeling approach is valid. Similar behavior in the scenario of nanofluid flow through pipes has been already reported in literature [32,42,46]. Hence, even though the slip velocity equation was valid for the particles in the order of micro and nanometers, the above assumption in SPM is sensible for the Reynolds number range considered in this study. But, there are also reports of non-uniform distribution of nanoparticles in the flow domain for nanofluids with larger nanoparticles and at different flow parameters [28].

5.2. Mean Nusselt number (Nu_M)

Fig. 4(a) and (b) illustrate the effects of nanoparticle volume fraction, Reynolds number and nanoparticle diameter on mean Nusselt number. As expected, the mean Nusselt number increases with increase in Reynolds number. As the flow velocity is increased, we observe a gradual increase in heat transfer. The mean Nusselt number is lowest at $Re = 10$ and has the maximum value at $Re = 40$. Addition of nanoparticles to the basefluid resulted in heat transfer augmentation which is understood by the increase in Nusselt number with increase of particle volume fraction. It can be clearly stated that the mean Nusselt number is higher for nanofluids than the basefluid at any given Reynolds number. This augmentation of heat transfer with increase in nanoparticle volume fraction can attributed to the increase in thermal conductivity of nanofluids with addition of nanoparticles. The increase in thermal conductivity leads to reduced thermal boundary layer thickness and delayed growth of boundary layer, which are clear indications of increased heat transfer rates. In addition to that, the mean Nusselt number is significantly influenced by the particle diameter. Increasing the nanoparticle size induced a deteriorating effect on heat transfer. The highest values of mean Nusselt number are noted at $d_p = 10\,\text{nm}$ and the lowest values are observed at $d_p = 50\,\text{nm}$ for any volume fraction and Reynolds number. For instance, 12% increase in mean Nusselt number is observed when the particle diameter is reduced from 50 nm to 10 nm at $\phi = 5\%$.

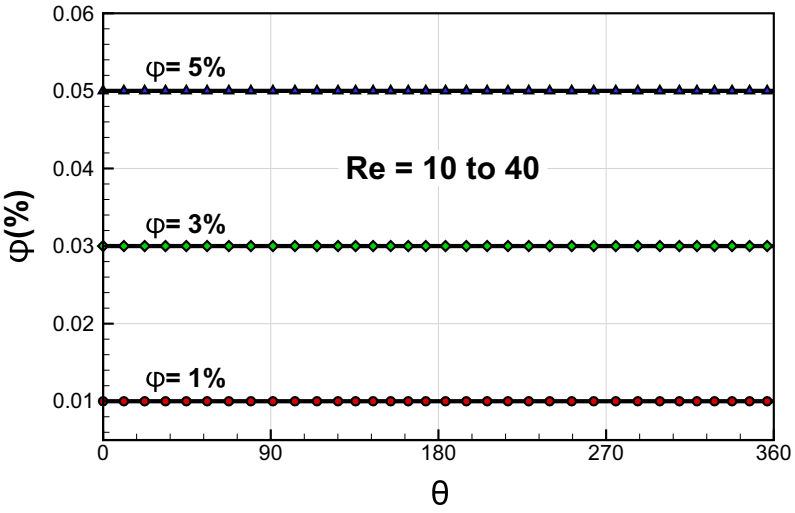

Fig. 3. Distribution of nanoparticles around the cylinder surface at $10 \leqslant Re \leqslant 40$ and 10 nm $\leqslant d_p \leqslant$ 50 nm using MPM.

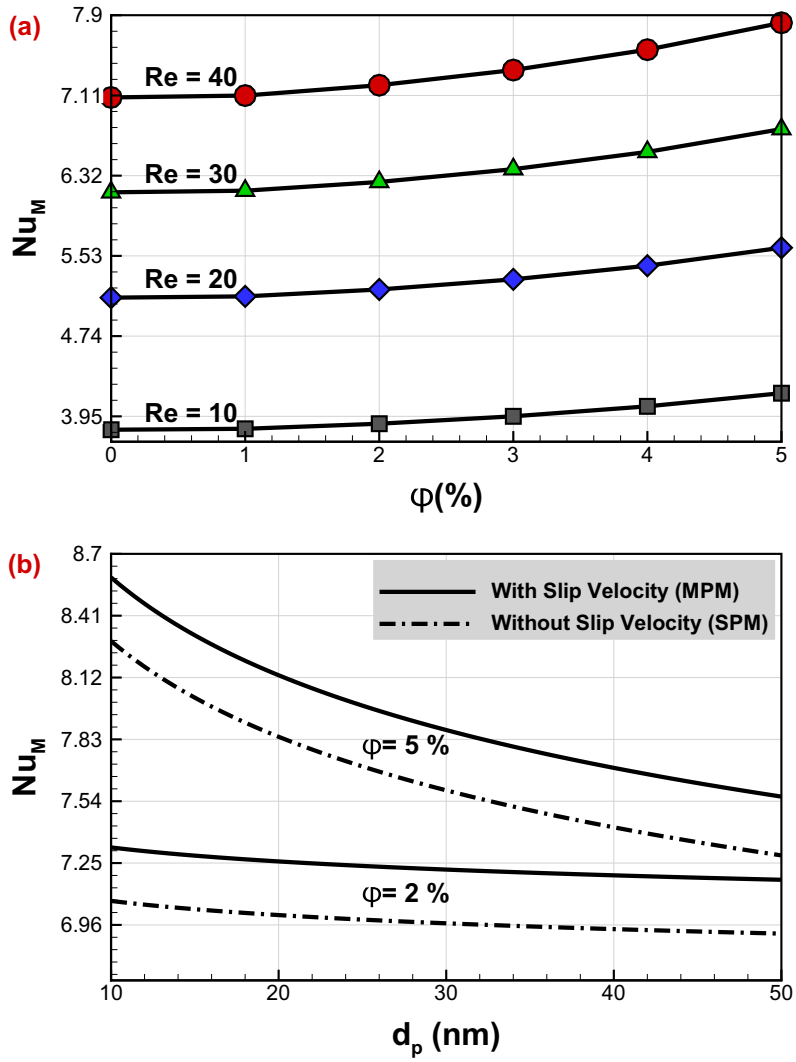

Fig. 4. (a) Variation of mean Nusselt number with particle volume fraction and Reynolds number using MPM and (b) Effects of slip velocity on mean Nusselt number at $10 \leqslant d_p \leqslant 50$ nm and $Re = 40$.

It can be concluded that 10 nm particle diameter is best for Al_2O_3–Water nanofluid to get high heat transfer rates. Smaller nanoparticles exhibit increased Brownian motion and hence, the interaction between fluid and particles will be more intense, leading to an increase in thermal transport. Furthermore, smaller the nanoparticles, higher will be the number of nanoparticles for a given volume fraction; which further leads to increased interaction between the fluid and nanoparticles. However, smaller particles, due to increased Brownian motion; may lead to higher degree of particle clustering and increase in viscosity. In overall, we can conclude that, that decreasing the particle size will result in increment of both viscosity and thermal conductivity of nanofluids with a net increase in mean Nusselt number.

5.3. Surface Nusselt number, (Nu_S)

Local distributions of Nusselt number along the cylinder surface at $Re = 10, 40$ and $\phi = 2\%, 5\%$ along with that of pure water are shown in Fig. 5(a) and (b). It is seen that the local Nusselt number values are highest at the front stagnation point and then gradually decrease towards the rear stagnation point. At $Re = 40$, we observe a slight increase in Nusselt number distribution at the rear stagnation point which can be attributed to the increased flow recirculation at $Re = 40$ when compared to $Re = 10$. The values of local Nusselt number increase with increase in particle volume fraction. This is because of the net increase in effective thermal conductivity of nanofluids with addition of nanoparticles. The increase in local Nusselt number distribution with increase in particle volume fraction is more pronounced near the front stagnation point. The local Nusselt number distribution is higher at higher Reynolds numbers due to increased flow velocities. In addition to the effects of particle volume fraction and Reynolds number, the local Nusselt number distribution is also enhanced by decreasing the particle diameter. The local Nusselt number distribution around the cylinder surface with $\phi = 2\%, 5\%$ and $d_p = 10$ nm,50 nm at $Re = 40$ are shown in Fig. 6(a) and (b). Even though higher Nusselt distribution is seen at $d_p = 10$ nm at all the volume fractions, the effect is more amplified at $\phi = 5\%$. This is because at higher particle volume fractions and smaller diameters, the number of nanoparticles are more. This leads to enhanced interaction between the particles and base-fluid which results in pronounced augmentation of Nusselt number.

5.4. Heat transfer enhancement ratio, (E)

Fig. 7(a) and (b) graphically show the effects of volume fractions, Reynolds number and nanoparticle diameter on E which is defined by Eq. (18). Irrespective of the Reynolds number, the values

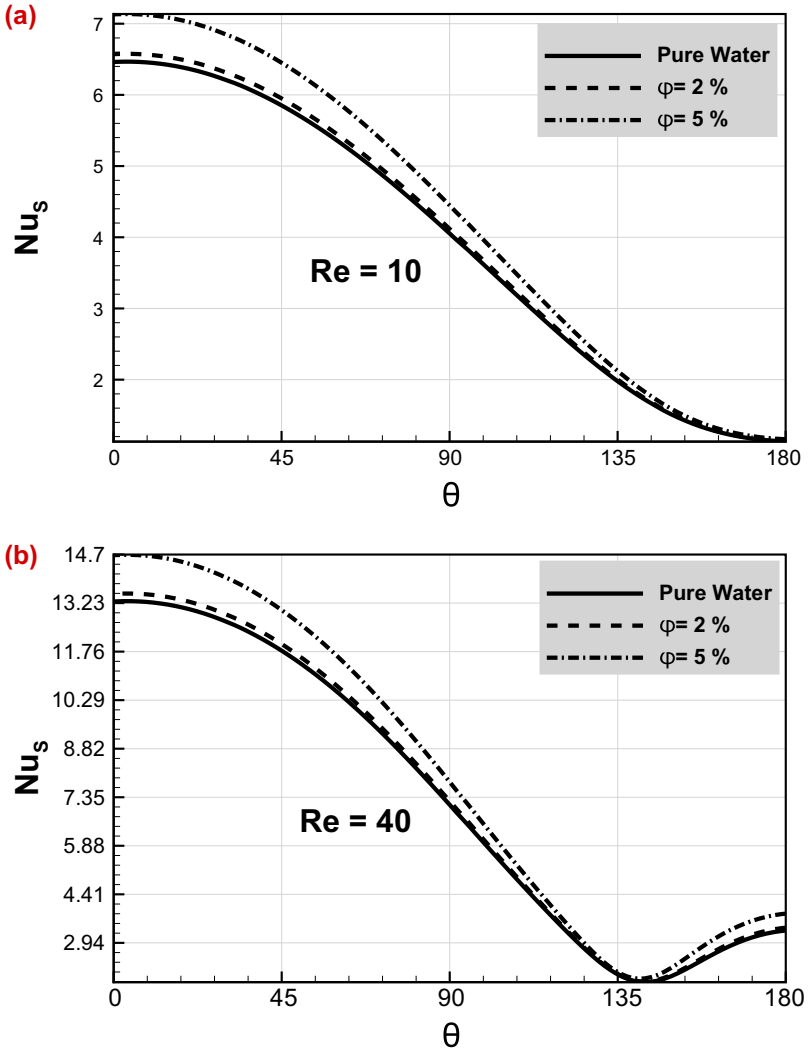

Fig. 5. Distribution of local Nusselt number over the cylinder surface using MPM at (a) $Re = 10$ and (b) $Re = 40$.

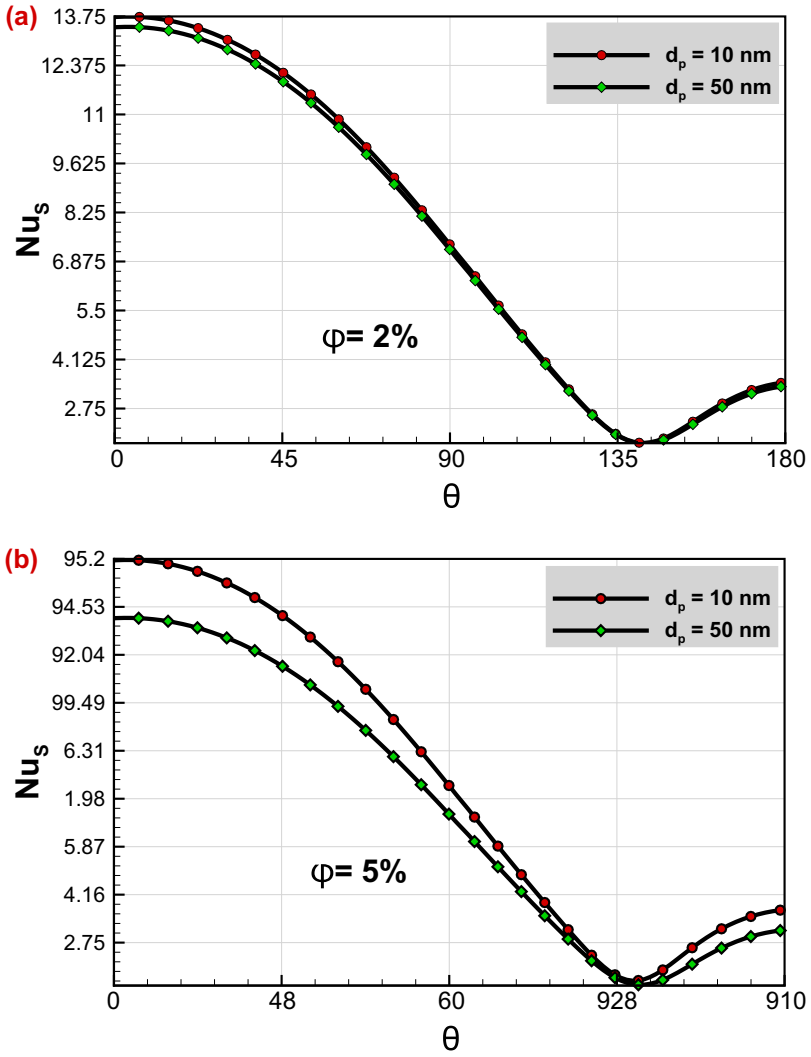

Fig. 6. Effects of particle diameter on local Nusselt number distribution over the cylinder surface at $Re = 40$ using MPM at (a) $\phi = 2\%$ and (b) $\phi = 5\%$.

of E increases with addition of nanoparticles. We can observe a monotonous increase in E with increase in nanoparticle volume fraction. This can be related to the increased Nusselt numbers at higher volume fractions, which is explained clearly in the above sections. Results indicate that the nanoparticle diameter is inversely proportional to the heat transfer augmentation. E decreases with increase in particle diameter at any given particle volume fraction and Reynolds number. This is due to the fall in effective thermal conductivity of nanofluids at larger particle diameters. The variations of E with respect to particle volume fraction, particle diameter and Reynolds number can be directly attributed to the variations observed in the mean Nusselt number. It can be concluded that, at any given volume fraction, nanofluids produce enhanced heat transfer than pure water. Also, smaller nanoparticles are capable of producing higher heat transfer rates at any given particle volume fraction and Reynolds number. In conclusion, the highest heat transfer enhancement ratio is observed for 5% nanofluid with 10 nm sized nanoparticles.

5.5. Isotherms

The effects of Reynolds number, particle volume fraction and nanoparticle diameter on the thermal field around the circular cylinder are visualized using isotherm patterns in Figs. 8–10. In general, the front surface of the cylinder has higher temperature gradients which is indicated by the maximum clustering of the temperature isotherms at the front surface. This can also be related with the high Nusselt number distribution seen at the front surface. It can be seen from Fig. 8(a) and (b), clustering of the isotherms increase with increase in Reynolds number. In the rear side of the cylinder, the clustering of the isotherms increase at higher Reynolds numbers due to increased recirculating wakes. Also, the thickness of the thermal boundary layer decreases with increase in Reynolds number indicating higher heat transfer rates. The complexity of the aft contours increases with increase in Reynolds numbers. At $Re = 10$, the temperature contours were more symmetric and simple. At $Re = 40$, we observe a thumb like projection of the thermal plume from the top and bottom surface of the cylinder, while the center part of the thermal plume gets closer to the rear stagnation point. Fig. 9(a) and (b), show the isotherm patterns at $\varnothing = 2\%$ and 5% at $Re = 40$. It can be seen that the thermal boundary thinning takes place with increase in particle volume fraction which indicates the higher heat transfer rates at higher volume fractions. At higher volume fractions, isotherms get more clustered and the thumb like projection of the thermal plume becomes more sharp and defined. This phenomena can be attributed to the increase in thermal conductivity of the nanofluids at higher volume fractions which leads to increased temperature

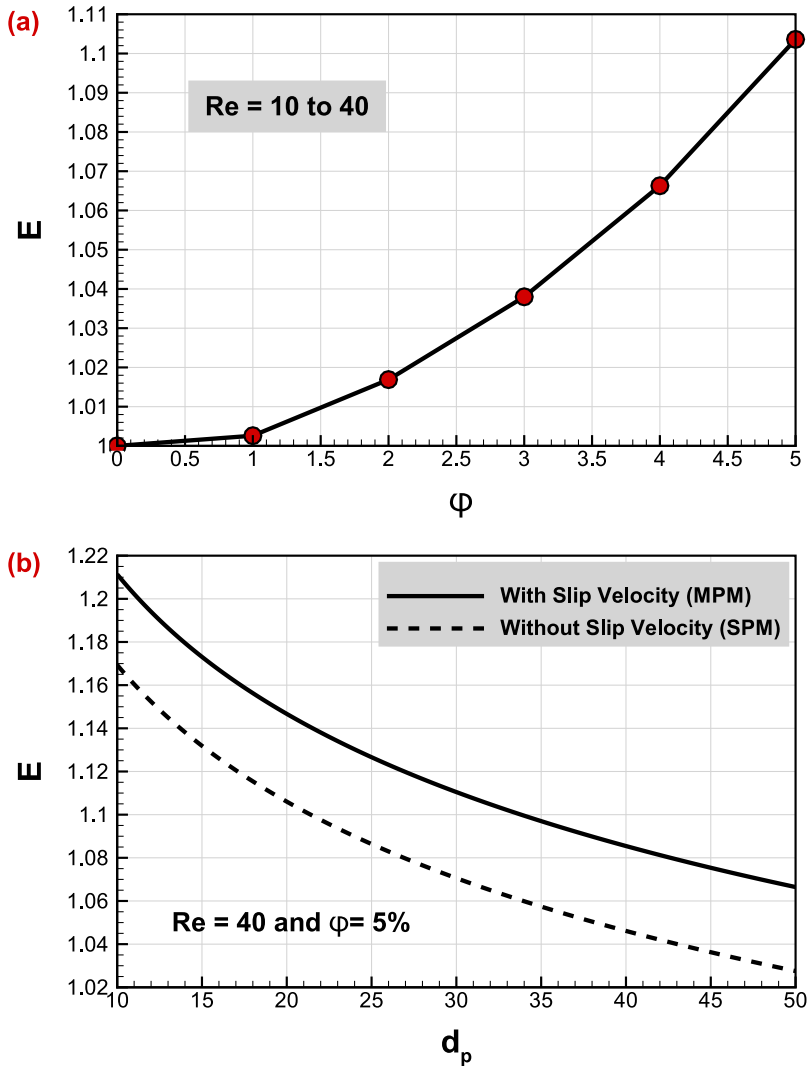

Fig. 7. (a) Heat transfer enhancement ratio (E) of nanofluids at different volume fractions and $Re = 40$ using MPM and (b) Effects of slip velocity on E at $10 \leqslant d_p \leqslant 50$ nm and $Re = 40$.

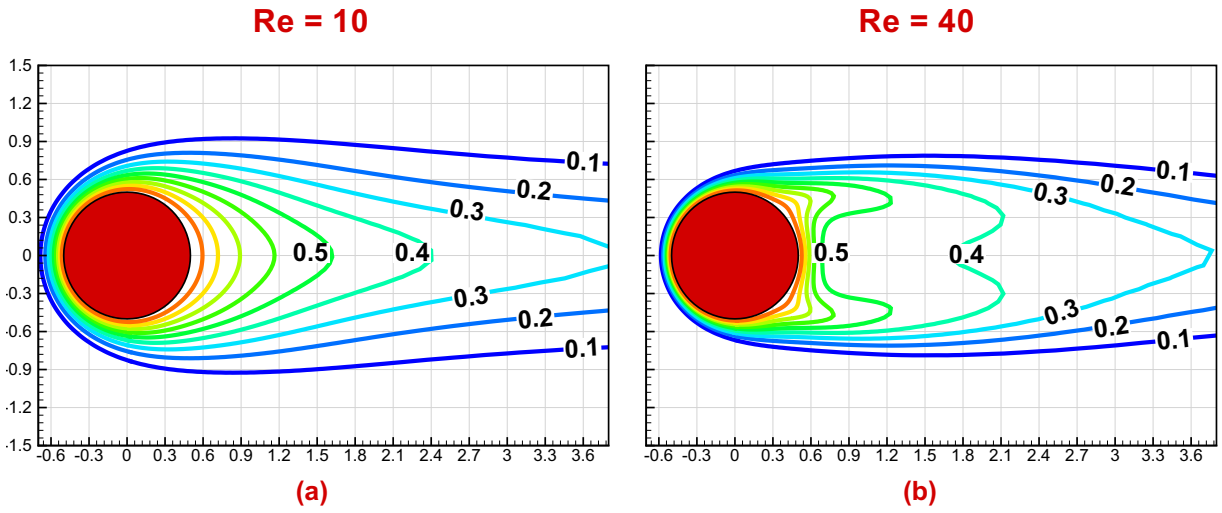

Fig. 8. Effects of Reynolds number on thermal field (isotherm pattern) around the circular cylinder at $\phi = 5\%$ and $d_p = 30$ nm using MPM.

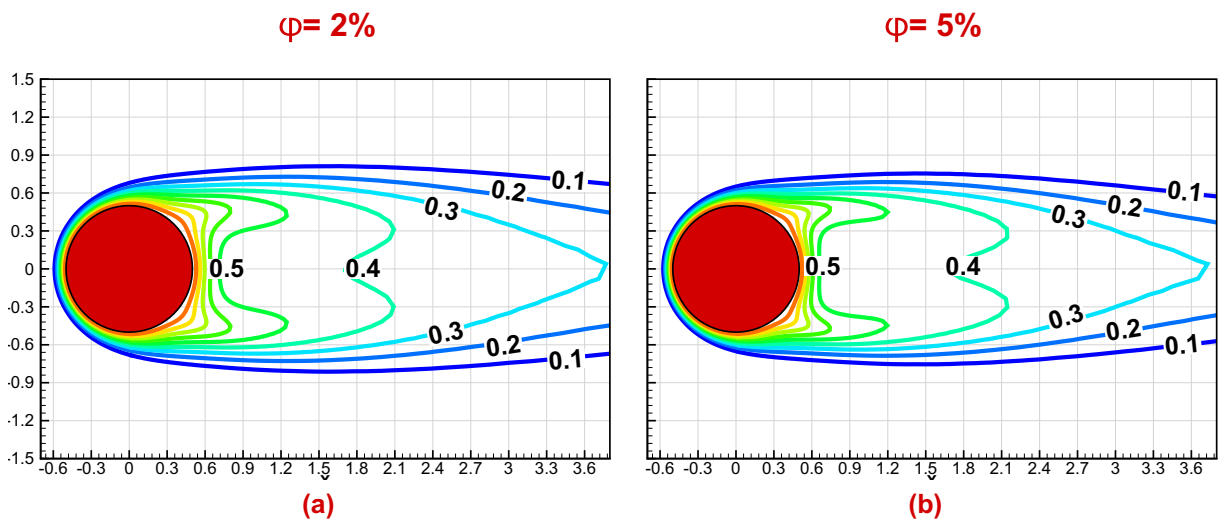

Fig. 9. Effects of particle volume fraction on thermal field (isotherm pattern) around the circular cylinder at $Re = 40$ and $d_p = 30$ nm using MPM.

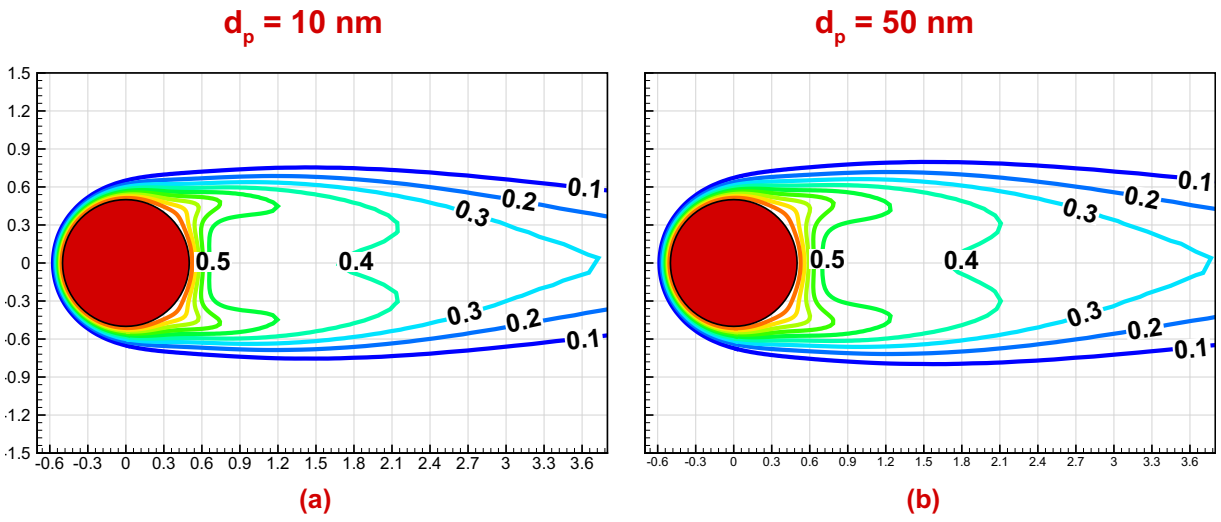

Fig. 10. Variation of thermal field (isotherm pattern) around the circular cylinder with particle diameter at $\phi = 5\%$ and $Re = 40$ using MPM.

gradients. The effect of particle diameter on the temperature distribution around the cylinder at $Re = 40$ and $\phi = 5\%$ is shown in Fig. 10(a) and (b). When the particle diameter is increased from 10 nm to 50 nm, the temperature gradient decreases which is indicated by the isotherms moving away from the cylinder. Also at higher particle diameters, the thermal boundary layer thickness increases indicating a deterioration in heat transfer. It can be concluded that higher volume fractions and Reynolds numbers along with smaller nanoparticles lead to augmentation of heat transfer.

5.6. Effects of slip velocity

The influence of modeling approach on mean Nusselt number is shown in Fig. 4(b) at $Re = 40$ and $\phi = 2\%, 5\%$. When the modeling approach is switched from SPM to MPM, an increase in mean Nusselt number is noticed. At a given Reynolds number and at any volume fraction, the heat transfer rates are higher when a mixture model based multi-phase approach is used. A similar effect is also seen in E which is shown in Fig. 7(b). Even though the heat transfer enhancement ratios of nanofluids are always greater than 1 at any ϕ, d_p and Re, its values are lower in SPM than in MPM. For instance, E at $\phi = 5\%, d_p = 50$ nm and $Re = 40$ using MPM is approximately 4% higher than that of SPM. The effects of modeling approach on the temperature distribution at $\phi = 5\%, d_p = 30$ nm and $Re = 40$ are shown in Fig. 11. It is seen that thermal boundary layer in MPM is thinner than that of the thermal boundary in SPM. This indicates augmented heat transfer rates in MPM than SPM. The isotherms of MPM are more closer and the thumb shape of the thermal plume is more defined indicating higher temperature gradients. In general, we can conclude that higher transfer rates are seen in MPM than SPM. This can be attributed to the slip velocity mechanisms considered in the mixture model based MPM. The MPM approach based on mixture model considers a non-zero slip velocity. Whereas, the SPM neglects the interaction between the particles and basefluid leading to lower heat transfer rates. Hence, it is realistic to achieve augmented heat transfer using MPM. Similar phenomena of increase in heat transfer when the modeling approach is switched from SPM to MPM was observed by Saha and Paul [42]. It should also be noted that, the difference in heat transfer between MPM and SPM is higher at higher particle volume fractions. This indicates that the interaction of particles and fluid become more significant at higher particle volume fractions. Thus,

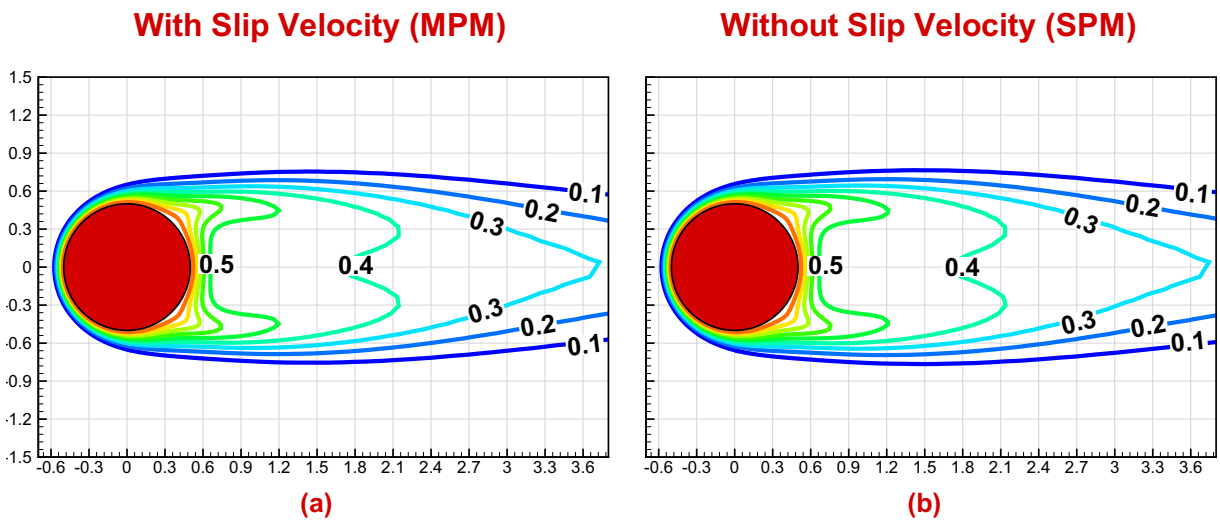

Fig. 11. Influence of slip velocity on thermal field (isotherm pattern) around the circular cylinder at $\phi = 5\%, d_p = 30$ nm and $Re = 40$.

we can say that the SPM approach may be suitable for small volume fractions. But at higher volume fractions, it is more meaningful and realistic to consider MPM for simulating nanofluid flow and heat transfer.

6. Conclusions and future work

Forced convective heat transfer around a 2-D circular cylinder during a steady, laminar flow of Al_2O_3–H_2O nanofluid has been numerically studied using a mixture model based Multi-Phase Modeling (MPM) approach. Effects of Reynolds number, particle volume fraction and diameter of nanoparticles on the heat transfer characteristics have been investigated. Special attention has been given to the change in heat transfer enhancement when the modeling approach is changed from SPM to MPM. Findings of the numerical investigation can be summarized as follows:

- Obviously, heat transfer is enhanced by increasing the Reynolds number.
- The mean Nusselt number is notably higher for nanofluids than the basefluid. For instance, the mean Nusselt at $Re = 40, \phi = 5\%$ and $d_p = 10$ nm nanofluid is approximately 18% higher than the basefluid (pure water).
- Particle diameters have significant enhancement on the heat transfer characteristics. Nanofluids with smaller nanoparticles resulted in augmentation of heat transfer and the effect of nanoparticle size is pronounced at higher volume fractions.
- Modeling approach is more important in numerically analyzing the behavior of nanofluids. MPM approach indicates higher heat transfer rates than the SPM approach.
- The difference in heat transfer between the two approaches is higher at higher volume fractions.
- Higher heat transfer rates seen in mixture model based MPM approach can be associated with the particle-fluid interactions due to slip velocity mechanisms such as Brownian motion and thermophoresis, etc.

Thus, we can conclude that the choice of modeling approach is very important while numerically analyzing nanofluid flow and heat transfer. The effects of slip velocity is more pronounced at higher volume fractions and is expected to be more influential in mixed and natural convective flow scenarios. Hence, in future a detailed study on natural and mixed convective heat transfer characteristics around a circular cylinder can be carried out using a mixture model based MPM approach.

Acknowledgments

One of the authors, S. Dhinakaran, gratefully acknowledges the financial aid received from Science and Engineering Research Board, Department of Science and Technology (DST), Government of India through a project Grant (Project Reference No. SB/FTP/ETA-427/2012) for carrying out this work. The authors are highly obliged to the reviewers for their insightful comments and suggestions.

References

[1] R.P. Bharti, R.P. Chhabra, V. Eswaran, Steady forced convection heat transfer from a heated circular cylinder to power-law fluids, Int. J. Heat Mass Transfer 50 (5) (2007) 977–990.
[2] R.A. Ahmad, Steady-state numerical solution of the Navier-Stokes and energy equations around a horizontal cylinder at moderate Reynolds numbers from 100 to 500, Heat Transfer Eng. 17 (1) (1996) 31–81.
[3] R.P. Chhabra, Bubbles, Drops, and Particles in Non-Newtonian Fluids, CRC press, 2006.
[4] R.P. Chhabra, Hydrodynamics of nonspherical particles in non-Newtonian fluids, Plast. Eng.-New York 31 (1996) 1–46.
[5] C.F. Lange, F. Durst, M. Breuer, Momentum and heat transfer from cylinders in laminar crossflow at $10^{-4} \leq Re \leq 200$, Int. J. Heat Mass Transfer 41 (22) (1998) 3409–3430.
[6] V.T. Morgan, The overall convective heat transfer from smooth circular cylinders, Adv. Heat Transfer 11 (1975) 199–264.
[7] C.H.K. Williamson, Vortex dynamics in the cylinder wake, Annu. Rev. Fluid Mech. 28 (1) (1996) 477–539.
[8] M.M. Zdravkovich, Flow around circular cylinders; vol. i fundamentals, J. Fluid Mech. 350 (1) (1997) 377–378.
[9] M.M. Zdravkovich, Flow Around Circular Cylinders, Vol. 2: Applications, vol. 19, Oxford University Press, 2003, ISBN 0, (856561), pp. 5.
[10] A. Zukauskas, Convective Heat Transfer in Cross Flow, vol. 6, Wiley, New York, 1987.
[11] G. Saha, M.C. Paul, Numerical analysis of the heat transfer behaviour of water based Al_2O_3 and TiO_2 nanofluids in a circular pipe under the turbulent flow condition, Int. Commun. Heat Mass Transfer 56 (2014) 96–108.
[12] M.S. Valipour, A.Z. Ghadi, Numerical investigation of fluid flow and heat transfer around a solid circular cylinder utilizing nanofluid, Int. Commun. Heat Mass Transfer 38 (9) (2011) 1296–1304.
[13] R.L. Hamilton, O.K. Crosser, Thermal conductivity of heterogeneous two-component systems, Ind. Eng. Chem. Fundam. 1 (3) (1962) 187–191.
[14] H.C. Brinkman, The viscosity of concentrated suspensions and solutions, J. Chem. Phys. 20 (4) (1952), 571–571.
[15] M.S. Valipour, R. Masoodi, S. Rashidi, M. Bovand, M. Mirhosseini, A numerical study on convection around a square cylinder using $Al_2O_3 - H_2O$ nanofluid, Therm. Sci. 18 (4) (2014) 1305–1314.

[16] M. Vegad, S. Satadia, P. Pradip, P. Chirag, P. Bhargav, Heat transfer characteristics of low Reynolds number flow of nanofluid around a heated circular cylinder, Procedia Technol. 14 (2014) 348–356.
[17] J.C.M. Garnett, Colours in metal glasses, in metallic films, and in metallic solutions. ii, Philos. Trans. R. Soc. London, Ser. A (1906) 237–288.
[18] E. Abu-Nada, K. Ziyad, M. Saleh, Y. Ali, Heat transfer enhancement in combined convection around a horizontal cylinder using nanofluids, J. Heat Transfer 130 (8) (2008) 084505.
[19] R.T.H. Bing, H.A. Mohammed, Upward laminar flow around a circular cylinder using nanofluids, J. Purity Util. React. Environ. 1 (2012) 435–450.
[20] V. Etminan-Farooji, E. Ebrahimnia-Bajestan, H. Niazmand, S. Wongwises, Unconfined laminar nanofluid flow and heat transfer around a square cylinder, Int. J. Heat Mass Transfer 55 (5) (2012) 1475–1485.
[21] A.J. Chamkha, A. Rashad, A.M. Aly, Transient natural convection flow of a nanofluid over a vertical cylinder, Meccanica 48 (1) (2013) 71–81.
[22] S. Sarkar, A. Dalal, G. Biswas, Unsteady wake dynamics and heat transfer in forced and mixed convection past a circular cylinder in cross flow for high prandtl numbers, Int. J. Heat Mass Transfer 54 (15) (2011) 3536–3551.
[23] S. Sarkar, S. Ganguly, G. Biswas, Mixed convective heat transfer of nanofluids past a circular cylinder in cross flow in unsteady regime, Int. J. Heat Mass Transfer 55 (17) (2012) 4783–4799.
[24] S. Sarkar, S. Ganguly, A. Dalal, Buoyancy driven flow and heat transfer of nanofluids past a square cylinder in vertically upward flow, Int. J. Heat Mass Transfer 59 (2013) 433–450.
[25] S. Sarkar, S. Ganguly, A. Dalal, P. Saha, S. Chakraborty, Mixed convective flow stability of nanofluids past a square cylinder by dynamic mode decomposition, Int. J. Heat Fluid Flow 44 (2013) 624–634.
[26] S. Sarkar, S. Ganguly, A. Dalal, Analysis of entropy generation during mixed convective heat transfer of nanofluids past a rotating circular cylinder, J. Heat Transfer 136 (6) (2014) 062501.
[27] Y. Xuan, Q. Li, Heat transfer enhancement of nanofluids, Int. J. Heat Fluid Flow 21 (1) (2000) 58–64.
[28] A. Akbarinia, R. Laur, Investigating the diameter of solid particles effects on a laminar nanofluid flow in a curved tube using a two phase approach, Int. J. Heat Fluid Flow 30 (4) (2009) 706–714.
[29] L.-S. Fan, C. Zhu, Principles of Gas-solid Flows, Cambridge University Press, 2005.
[30] D. Gidaspow, Multiphase Fflow and Fluidization: Continuum and Kinetic Theory Descriptions, Academic press, 1994.
[31] M. Manninen, V. Taivassalo, S. Kallio, et al., On the mixture model for multiphase flow (1996).
[32] A. Behzadmehr, M. Saffar-Avval, N. Galanis, Prediction of turbulent forced convection of a nanofluid in a tube with uniform heat flux using a two phase approach, Int. J. Heat Fluid Flow 28 (2) (2007) 211–219.
[33] M. Alinia, D.D. Ganji, M. Gorji-Bandpy, Numerical study of mixed convection in an inclined two sided lid driven cavity filled with nanofluid using two-phase mixture model, Int. Commun. Heat Mass Transfer 38 (10) (2011) 1428–1435.
[34] M. Esfandiary, B. Mehmandoust, A. Karimipour, H.A. Pakravan, Natural convection of Al_2O_3–water nanofluid in an inclined enclosure with the effects of slip velocity mechanisms: Brownian motion and thermophoresis phenomenon, Int. J. Therm. Sci. 105 (2016) 137–158.
[35] O. Ghaffari, A. Behzadmehr, H. Ajam, Turbulent mixed convection of a nanofluid in a horizontal curved tube using a two-phase approach, Int. Commun. Heat Mass Transfer 37 (10) (2010) 1551–1558.
[36] F. Vahidinia, M. Rahmdel, Turbulent mixed convection of a nanofluid in a horizontal circular tube with non-uniform wall heat flux using a two-phase approach, Transp. Phenom. Nano Micro Scales 3 (2) (2015) 106–117.
[37] M. Goodarzi, M.R. Safaei, K. Vafai, G. Ahmadi, M. Dahari, S.N. Kazi, N. Jomhari, Investigation of nanofluid mixed convection in a shallow cavity using a two-phase mixture model, Int. J. Therm. Sci. 75 (2014) 204–220.
[38] R. Lotfi, Y. Saboohi, A.M. Rashidi, Numerical study of forced convective heat transfer of nanofluids: comparison of different approaches, Int. Commun. Heat Mass Transfer 37 (1) (2010) 74–78.
[39] S. Mirmasoumi, A. Behzadmehr, Numerical study of laminar mixed convection of a nanofluid in a horizontal tube using two-phase mixture model, Appl. Therm. Eng. 28 (7) (2008) 717–727.
[40] R.M. Moghari, A. Akbarinia, M. Shariat, F. Talebi, R. Laur, Two phase mixed convection Al_2O_3-water nanofluid flow in an annulus, Int. J. Multiph. Flow 37 (6) (2011) 585–595.
[41] H.A. Pakravan, M. Yaghoubi, Analysis of nanoparticles migration on natural convective heat transfer of nanofluids, Int. J. Therm. Sci. 68 (2013) 79–93.
[42] G. Saha, M.C. Paul, Heat transfer and entropy generation of turbulent forced convection flow of nanofluids in a heated pipe, Int. Commun. Heat Mass Transfer 61 (2015) 26–36.
[43] M. Siavashi, M. Jamali, Heat transfer and entropy generation analysis of turbulent flow of TiO_2–water nanofluid inside annuli with different radius ratios using two-phase mixture model, Appl. Therm. Eng. 100 (2016) 1149–1160.
[44] M.H. Fard, M.N. Esfahany, M. Talaie, Numerical study of convective heat transfer of nanofluids in a circular tube two-phase model versus single-phase model, Int. Commun. Heat Mass Transfer 37 (1) (2010) 91–97.
[45] M. Kalteh, A. Abbassi, M. Saffar-Avval, J. Harting, Eulerian–eulerian two-phase numerical simulation of nanofluid laminar forced convection in a microchannel, Int. J. Heat Fluid Flow 32 (1) (2011) 107–116.
[46] V. Bianco, F. Chiacchio, O. Manca, S. Nardini, Numerical investigation of nanofluids forced convection in circular tubes, Appl. Therm. Eng. 29 (17) (2009) 3632–3642.
[47] S.Z. Heris, M.N. Esfahany, G. Etemad, Numerical investigation of nanofluid laminar convective heat transfer through a circular tube, Numer. Heat Transfer, Part A: Appl. 52 (11) (2007) 1043–1058.
[48] S. Rashidi, M. Bovand, J.A. Esfahani, G. Ahmadi, Discrete particle model for convective Al_2O_3–water nanofluid around a triangular obstacle, Appl. Therm. Eng. 100 (2016) 39–54.
[49] M. Akbari, N. Galanis, A. Behzadmehr, Comparative assessment of single and two-phase models for numerical studies of nanofluid turbulent forced convection, Int. J. Heat Fluid Flow 37 (2012) 136–146.
[50] S. Göktepe, K. Atalık, H. Ertürk, Comparison of single and two-phase models for nanofluid convection at the entrance of a uniformly heated tube, Int. J. Therm. Sci. 80 (2014) 83–92.
[51] M.K. Moraveji, R.M. Ardehali, CFD modeling (comparing single and two-phase approaches) on thermal performance of Al_2O_3/water nanofluid in mini-channel heat sink, Int. Commun. Heat Mass Transfer 44 (2013) 157–164.
[52] M. Ishii, Thermo-fluid dynamic theory of two-phase flow, NASA STI/Recon Technical Report A 75 (1975) 29657.
[53] C.T. Crowe, T.R. Troutt, J.N. Chung, Numerical models for two-phase turbulent flows, Annu. Rev. Fluid Mech. 28 (1) (1996) 11–43.
[54] J. Xu, A. Rouelle, K.M. Smith, D. Celik, M.Y. Hussaini, S.W. Van Sciver, Two-phase flow of solid hydrogen particles and liquid helium, Cryogenics 44 (6) (2004) 459–466.
[55] S. Kakaç, A. Pramuanjaroenkij, Single-phase and two-phase treatments of convective heat transfer enhancement with nanofluids–A state-of-the-art review, Int. J. Therm. Sci. 100 (2016) 75–97.
[56] N.A.C. Sidik, M.N.A.W.M. Yazid, S. Samion, M.N. Musa, R. Mamat, Latest development on computational approaches for nanofluid flow modeling: Navier–Stokes based multiphase models, Int. Commun. Heat Mass Transfer 74 (2016) 114–124.
[57] H. El-Batsh, M. Doheim, A. Hassan, On the application of mixture model for two-phase flow induced corrosion in a complex pipeline configuration, Appl. Math. Model. 36 (11) (2012) 5686–5699.
[58] A. FLUENT, 6.3, 2006, fluent 6.3 users guide, fluent, Inc., Lebanon, NH.
[59] L. Schiller, Z. Naumann, A drag coefficient correlation, Vdi Zeitung 77 (318) (1935) 51.
[60] A. Sohankar, C. Norberg, L. Davidson, Low-Reynolds-number flow around a square cylinder at incidence: study of blockage, onset of vortex shedding and outlet boundary condition, Int. J. Numer. Methods Fluids 26 (1) (1998) 39–56.
[61] J. Buongiorno, Convective transport in nanofluids, J. Heat Transfer 128 (3) (2006) 240–250.
[62] M. Corcione, Empirical correlating equations for predicting the effective thermal conductivity and dynamic viscosity of nanofluids, Energy Convers. Manage. 52 (1) (2011) 789–793.
[63] S.C.R. Dennis, G.-Z. Chang, Numerical solutions for steady flow past a circular cylinder at Reynolds numbers up to 100, J. Fluid Mech. 42 (3) (1970) 471–489.
[64] A.A. Soares, J.M. Ferreira, R.P. Chhabra, Flow and forced convection heat transfer in crossflow of non-Newtonian fluids over a circular cylinder, Ind. Eng. Chem. Res. 44 (15) (2005) 5815–5827.